Inorganic Chemistry

Article

6-(3,5-Dimethyl-1*H*-pyrazol-1-yl)-2,2′-bipyridine as Ligand
for Actinide(III)/Lanthanide(III) Separation

Denise Girnt,[†] **Peter W. Roesky,**[*,†] **Andreas Geist,**[‡] **Christian M. Ruff,**[§] **Petra J. Panak,**[§] **and Melissa A. Denecke**[‡]

[†]*Institut für Anorganische Chemie, Karlsruher Institut für Technologie (KIT), Engesserstrasse 15, 76131 Karlsruhe, Germany,* [‡]*Institut für Nukleare Entsorgung, Karlsruher Institut für Technologie (KIT), P.O. Box 3640, 76021 Karlsruhe, Germany, and* [§]*Institut für Physikalische Chemie, Ruprecht-Karls-Universität Heidelberg, Im Neuenheimer Feld 253, 69120 Heidelberg, Germany*

With the aim of better understanding the selectivity of the established system 2,6-ditriazinylpyridine (BTP) for actinide(III)/lanthanide(III) separations, a related model system was synthesized and studied. The *N* donor complexing ligand 6-(3,5-dimethyl-1*H*-pyrazol-1-yl)-2,2′-bipyridine (dmpbipy) was synthesized having a fused *N* heterocycle ring structure modified from the BTP partitioning ligand, and its extraction performance and selectivity for trivalent actinide cations over lanthanides was evaluated. X-ray diffraction (XRD), extended X-ray absorption fine structure (EXAFS), and time-resolved laser fluorescence spectroscopy (TRLFS) results show that 1:1 complexes are formed, unlike the 1:3 complex for BTP systems. The equilibrium constant for curium complex formation with dmpbipy was determined to be log K = 2.80, similar to that for nitrate. The Gibbs free energy, ΔG(20 °C), of 1:1 Cm-dmpbipy formation in *n*-octan-1-ol was measured to be −15.5 kJ/mol. The dmpbipy ligand in 1-octanol does not extract Am(III) Eu(III) from HNO_3 but was found to extract Am(III) with limited selectivity over Eu(III) ($SF_{Am(III)/Eu(III)} \approx 8$) dissolved in 2-bromohexanoic acid and kerosene at pH > 2.4.

Introduction

Partitioning and transmutation (P&T) is one strategy to reduce the long-term radiotoxicity of waste generated from nuclear power production presently subject of international research.[1,2] The basic idea is separation of the minor actinide elements (MA = Np, Am, and Cm), which together with plutonium are mainly responsible for the long-term toxicity of nuclear waste, from the waste and converting them by neutron fission (transmutation) into shorter-lived or stable elements. This strategy necessitates separation of MA from chemically similar lanthanides (Ln) and fission products in a process called partitioning. Development of a partitioning process with sufficient selectivity, which can perform separations under process conditions such as low pH and high radiation fields, is a major scientific and technical challenge. To date, one of the most promising processes is chemical liquid−liquid extraction using complexation ligands with

donor atoms such as nitrogen or sulfur with higher affinity for trivalent MA over Ln(III).[3−6]

Alkylated 2,6-ditriazinylpyridines (BTPs, Scheme 1) were the first *N* donor extractants reported to selectively extract Am(III) and Cm(III) over Ln(III) cations under acidic conditions (1 M nitric acid).[7,8] Despite recent progress in our grasp of the selectivity of this extracting agent,[9−12] the level of understanding of BTPs selectivity on a molecular level is insufficient to target the design of new, more efficient, and selective partitioning reagents or fine-tune partitioning

---

*To whom correspondence should be addressed. E-mail: roesky@kit.edu.

(1) *Status and Assessment Report on Actinide and Fission Product Partitioning and Transmutation*; OECD-NEA, Paris, 1999.

(2) Magill, J.; Berthou, V.; Haas, D.; Galy, J.; Schenkel, R.; Wiese, H.-W.; Heusener, G.; Tommasi, J.; Youinou, G. *Nuclear Energy* **2003**, *42*, 263–277.

(3) Kolarik, Z. *Chem. Rev.* **2008**, *108*, 4208–4252 and references therein.

(4) Madic, C.; Boullis, B.; Baron, P.; Testard, F.; Hudson, M. J.; Liljenzin, J.-O.; Christiansen, B.; Ferrando, M.; Facchini, A.; Geist, A.; Modolo, G.; Espartero, A. G.; De Mendoza, J. *J. Alloys Compd.* **2007**, *444−445*, 23–27.

(5) Ekberg, C.; Fermvik, A.; Retegan, T.; Skarnemark, G.; Foreman, M. R. S.; Hudson, M. J.; Englund, S.; Nilsson, M. *Radiochim. Acta* **2008**, *96*, 225–233.

(6) Lewis, F. W.; Harwood, L. M.; Hudson, M. J.; Drew, M. G. B.; Modolo, G.; Sypula, M.; Desreux, J. F.; Bouslimani, N.; Vidick, G. *Dalton Trans.* **2010**, *39*, 5172–5182.

(7) Kolarik, Z.; Müllich, U.; Gassner, F. *Solv. Extr. Ion Exch.* **1999**, *17*, 23–32.

(8) Kolarik, Z.; Müllich, U.; Gassner, F. *Solv. Extr. Ion Exch.* **1999**, *17*, 1155–1170.

(9) Denecke, M. A.; Panak, P. J.; Burdet, F.; Weigl, M.; Geist, A.; Klenze, R.; Mazzanti, M.; Gompper, K. *C. R. Chim.* **2007**, *10*, 872–882.

(10) Denecke, M. A.; Rossberg, A.; Panak, P. J.; Weigl, M.; Schimmelpfennig, B.; Geist, A. *Inorg. Chem.* **2005**, *44*, 8418–8425.

(11) Iveson, P. B.; Rivière, C.; Guillaneux, D.; Nierlich, M.; Thuéry, P.; Ephritikhine, M.; Madic, C. *Chem. Commun.* **2001**, 1512–1513.

(12) Madic, C.; Hudson, M. J.; Liljenzin, J.-O.; Glatz, J.-P.; Nannicini, R.; Facchini, A.; Kolarik, Z.; Odoj, R. New Partitioning Techniques for Minor Actinides; EUR 19149, European Commission, Luxembourg, 2000.

Scheme 1
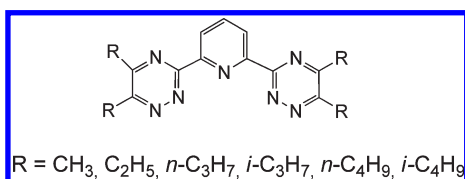
process conditions. Such advances are presently empirical, on a trial and error basis.

For this reasons we endeavored to make minor modifications on the BTP ligand system, to specifically study the influence of ligand geometry on coordination behavior and on the metal complex geometry and stability in hopes of shedding light onto the underlying driving force for BTP extraction selectivity. As a new ligand we report here on 6-(3,5-dimethyl-1*H*-pyrazol-1-yl)-2,2′-bipyridine (dmpbipy), a complexing ligand with only a limited number of modifications compared to BTP. Similar to BTP, dmpbipy consists of three fused aromatic *N* heterocycles. In contrast to BTP, however, one of these heterocycles is the five membered ring pyrazole. In addition to this modification of ring size (five versus six membered ring) dmpbipy also possesses a decreased number of nitrogen atoms in the heterocycle (pyridine vs 1,2,4-triazine). In the following, the synthesis of this ligand and its complexes with europium and samarium are described. The equilibrium constant, Gibbs free energy, enthalpy, and entropy of reaction for the curium dmpbipy complex formation were determined by time-resolved laser fluorescence spectroscopy (TRLFS). Finally results for liquid−liquid extraction studies for Am(III) and Eu(III) and for extended X-ray absorption fine structure (EXAFS) characterization of their coordination structure are discussed.

Experimental Section

Instrumentation and Measurements. NMR spectra were recorded on a Bruker Avance 400 MHz or a Bruker Avance II 300 MHz spectrometer. Chemical shifts are referenced to internal solvent resonances and are reported relative to tetramethylsilane (^{1}H NMR). IR spectra were obtained on a Bruker Tensor 37 FT-IR. Mass spectra were recorded at 70 eV on Varian Mat SM 11. Elemental analyses were carried out with an Elementar vario EL or vario MICRO cube.

TRLFS measurements were performed using an excimer pumped dye laser system (Lambda Physics, EMG 201 and FL 3002). A wavelength of 396.6 nm was used for excitation of Cm(III). Emission spectra were recorded from 580 to 620 nm using a delay time of 1.2 μs and a gate width of 1.3 ms. The fluorescence emission was detected by an optical multichannel analyzer consisting of a polychromator (Jobin Yvon, HR 320) with a 1200 lines/mm grating and an intensified photodiode array (Spectroscopy instruments, ST 180, IRY 700G). Details on the experimental setup are given elsewhere.[13] All measurements are performed at T = 20 °C, if not stated otherwise.

Syntheses. All manipulations of air-sensitive materials were performed with the rigorous exclusion of oxygen and moisture in flame-dried Schlenk-type glassware either on a dual manifold Schlenk line, interfaced to a high vacuum (10^{-3} Torr) line, or in an argon-filled MBraun glovebox. Diglyme and diethylether were distilled under nitrogen from potassium benzophenone

ketyl prior to use. K{(3,5-Me$_2$pz)(THF)}[14] was prepared according to literature procedure. Deuterated solvents were obtained from Aldrich (99 atom % D).

6-(3,5-Dimethyl-1*H*-pyrazol-1-yl)-2,2′-bipyridine (dmpbipy). The synthesis of 6-(3,5-dimethyl-1*H*-pyrazol-1-yl)-2,2′-bipyridine (dmpbipy) was performed according to the procedure reported by Steel et al.,[15] and the potassium-salt of the pyrazolate was prepared by the literature from Winter et al.[14]

A 0.44 g portion (3.3 mmol) of K{(3,5-Me$_2$pz)(THF)} and 1.04 g (4.4 mmol) of 6-bromo-2,2′-bipyridine were dissolved in 25 mL of diglyme under nitrogen. The yellow reaction solution was refluxed for 120 h. After 48 h the formation of solid potassium bromide was observed. Then the solvent was removed, and the white crude product was dissolved in 20 mL of diethylether. The undissolved solid was removed by filtration. After a second filtration with 20 mL of diethylether, the solvent was removed in vacuo and a white solid was obtained, which was recrystallized from *n*-pentane to give dmpbipy as analytical pure product. Yield: 0.67 g, 2.68 mmol, 81%. Single crystals were obtained by crystallization from *n*-pentane. ^{1}H NMR (CDCl$_3$, 400.1 MHz, 25 °C): δ = 2.29 (s, 3H, Me$_O$), 2.75 (s, 3H, Me$_N$), 5.99 (brs, 1H, H$_L$), 7.26 (dd, J^3(H$_B$H$_C$) = 7.5 Hz, J^4(H$_B$H$_D$) = 1.2 Hz, 1H, H$_B$), 7.59 (t, J^3(H$_C$H$_D$) = 7.8 Hz, 1H, H$_C$), 7.86 (d, J^3(H$_H$H$_G$) = 8.1 Hz, 1H, H$_H$), 7.89 (dd, J^3(H$_I$H$_H$) = 8.2 Hz, J^4(H$_I$H$_G$) = 1.6 Hz, 1H, H$_I$), 8.32 (dd, J^3(H$_D$H$_C$) = 7.8 Hz, J^4(H$_D$H$_B$) = 1.2 Hz, 1H, H$_D$), 8.34 (dd, J^3(H$_G$H$_H$) = 8.1 Hz, J^4(H$_G$H$_I$) = 1.6 Hz, 1H, H$_G$), 8.53 (dq, J^3(H$_A$H$_B$) = 4.8 Hz, J^4(H$_A$H$_C$) = 1.8 Hz, J^5(H$_A$H$_D$) = 0.9 Hz, 1H, H$_A$) ppm. ^{13}C{^{1}H} NMR (CDCl$_3$, 100.6 MHz, 25 °C): δ = 13.7 C$_O$, 15.2 C$_N$, 109.2 C$_L$, 115.6 C$_I$, 117.7 C$_G$, 121.0 C$_D$, 123.1 C$_B$, 136.9 C$_C$, 139.3 C$_H$, 141.3 C$_K$, 149.1 C$_M$, 149.2 C$_A$, 149.8 C$_J$, 154.4 C$_E$, 157.3 C$_F$ ppm.

The NMR spectra are in accordance with the literature.[15,16]
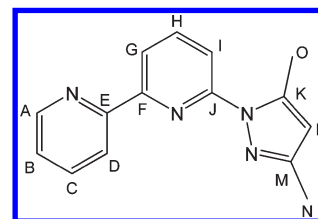
[Sm(dmpbipy)(NO$_3$)$_3$(DMSO)] (1). dmpbipy (310 mg, 1.24 mmol) and [Sm(NO$_3$)$_3$·6H$_2$O] (183 mg, 0.41 mmol) were dissolved in 10 mL of DMSO and refluxed for 24 h. After removal of the solvent, the white precipitate was recrystallized from hot ethanol to yield colorless crystals of **1**. Yield: 205 mg, 0.31 mmol, 75%. ^{1}H NMR (DMSO-d_6, 400.1 MHz, 22.0 °C): δ = 2.20 (s, 3H, Me$_O$), 2.54 (s, 6H, OS(Me$_2$)$_3$), 2.73 (s, 3H, Me$_N$), 6.15 (s, 1H, Me$_L$), 7.46 (dd, J^3(H$_B$H$_C$) = 7.7 Hz, J^3(H$_B$H$_A$) = 4.8 Hz 1H, H$_B$), 7.86 (d, J^3(H$_G$H$_H$) = 8.0 Hz, 1H, H$_G$), 7.97 (dt, J^3(H$_C$H$_B$) = 7.7 Hz, J^4(H$_C$H$_A$) = 1.8 Hz, 1H, H$_C$), 8.05 (t, J^3(H$_H$H$_I$) = 8.0 Hz, 1H, H$_H$), 8.25 (d, J^3(H$_D$H$_C$) = 7.7 Hz, 1H, H$_D$), 8.29 (d, J^3(H$_I$H$_H$) = 8.0 Hz, 1H, H$_I$), 8.69 (d, J^3(H$_A$H$_B$) = 4.8 Hz 1H, H$_A$) ppm. ^{13}C{^{1}H} NMR (DMSO-d_6, 100.6 MHz, 22.5 °C): δ = 13.6 C$_O$, 15.1 C$_N$, 40.4 OS(Me$_3$)$_2$, 109.6 C$_L$, 115.38 C$_I$, 117.6 C$_D$, 120.8 C$_B$, 124.7 C$_G$, 137.8 C$_C$, 140.3 C$_H$, 141.0 C$_K$, 149.3 C$_M$, 149.6 C$_A$, 150.0 C$_J$, 152.8 C$_E$, 154.8 C$_F$ ppm. IR (ν/cm^{-1}): 3627 (w), 3184 (w), 2925 (w), 2858 (w), 2496 (w), 2159 (w), 2025 (w), 1974 (w), 1742 (w), 1599 (s), 1560 (s), 1457 (w), 1360 (w), 1287 (s), 1069 (s), 1030 (s), 996 (s), 959 (s), 815 (s), 777 (s), 735 (s), 681 (s), 648 (w). EI/MS (70 eV, 180 °C) *m/z* (%): 576 (M$^+$ − 3 NO, 0.3), 565 (0.4), 551 (1.4), 463 (M$^+$ − 2 NO$_3$, DMSO, 0.5), 250 (dmpbipy, 71), 235 (46), 222 (12), 209 (40), 171 (17), 156 (95), 78 (100), 62 (NO$_3$, 68), 48 (27),

(13) Chung, K. H.; Klenze, R.; Park, K. K.; Paviet-Hartmann, P.; Kim, J. I. *Radiochim. Acta* **1998**, *82*, 215–219.

(14) Yelamos, C.; Heeg, M. J.; Winter, C. H. *Inorg. Chem.* **1998**, *37*, 3892–3894.

(15) Downard, A. J.; Honey, G. E.; Steel, P. J. *Inorg. Chem.* **1991**, *30*, 3733–3737.

(16) Gelling, A.; Orrell, K. G.; Osborne, A. G.; Šik, V. *J. Chem. Soc., Dalton Trans.* **1994**, 3545–3552.

30 (6). (**1**) $C_{17}H_{20}N_7O_{10}S$ (664.81): calcd. C, 30.71, H, 3.03, N, 14.75; found C, 30.64, H, 3.10, N, 14.35%.

[Eu(dmpbipy)(NO$_3$)$_3$(H$_2$O)]·(2). dmpbipy (290 mg, 1.15 mmol) and [Eu(NO$_3$)$_3$·6H$_2$O] (172 mg, 0.43 mmol) were suspended in 10 mL of dichloromethane, 5 mL of THF, and 5 mL of ethanol. The reaction mixture was stirred for 12 h at 45 °C. Colorless crystals **2** were obtained a few days after filtration from the mother liquor. Yield: 115 mg, 0.19 mmol, 45%. ^{1}H NMR (CD$_3$CN, 300.1 MHz, 23.0 °C): δ = 2.25 (br, 3H, Me$_O$), 2.77 (br, 3H, Me$_N$), 6.10 (br, 1H, H$_L$), 7.41 (m, 1H, H$_B$), 7.88−7.99 (m, 3H, H$_G$, H$_C$, H$_H$), 8.27−8.38 (m, 2H, H$_I$, H$_D$), 8.68 (m, 1H, H$_A$) ppm. IR (ν/cm^{-1}): 2962 (s), 2523 (w), 2159 (w), 2029 (w), 1975 (w), 1563 (w), 1455 (w), 1308 (w), 1258 (s), 1009 (s), 863 (s), 789 (s), 700 (s), 684 (s), 661 (s).

X-ray Crystallographic Studies of dmpbipy and 1−2. Crystals of dmpbipy were grown from *n*-pentane, crystals of **1** were obtained from ethanol, and crystals of **2** were grown from the mother liquor. A suitable crystal of compounds **1** and **2** was covered in mineral oil (Aldrich) and mounted onto a glass fiber. The crystal was transferred directly to the −73 °C N$_2$ cold stream of a Stoe IPDS 2 diffractometer. Subsequent computations were carried out on an Intel Pentium Core2Duo.

All structures were solved by the Patterson method (SHELXS-97).[17] The remaining non-hydrogen atoms were located from successive difference Fourier map calculations. The refinements were carried out by using full-matrix least-squares techniques on F, minimizing the function $(F_o - F_c)^2$, where the weight is defined as $4F_0^2/2(F_o^2)$ and F_o and F_c are the observed and calculated structure factor amplitudes, using the program SHELXL-97.[17] Carbon-bound hydrogen atom positions were calculated and allowed to ride on the carbon to which they are bonded. The hydrogen atom contributions of compounds **1** and **2** were calculated, but not refined. The locations of the largest peaks in the final difference Fourier map calculation as well as the magnitude of the residual electron densities in each case were of no chemical significance.

Crystal data for dmpbipy: $C_{15}H_{14}N_4$, $M = 250.30$, orthorhombic, $a = 5.0833(10)$ Å, $b = 14.957(3)$ Å, $c = 16.451(3)$ Å, $V = 1250.8(4)$ Å^3, $T = 150(2)$ K, space group $P2_12_12_1$, $Z = 4$, μ(MoKα) = 0.083 mm^{-1}, 3392 reflections measured, 2508 independent reflections (R_{int} = 0.0389). The final R_1 values were 0.0383 ($I > 2\sigma(I)$). The final $wR(F^2)$ values were 0.0994 (all data). The goodness of fit on F^2 was 1.022.

Crystal data for **1**: $C_{17}H_{20}N_7O_{10}SSm$, $M = 664.81$, triclinic, $a = 9.4637(19)$ Å, $b = 10.825(2)$ Å, $c = 11.554(2)$ Å, $\alpha = 85.30(3)°$, $\beta = 86.30(3)°$, $\gamma = 88.61(3)°$, $V = 1176.9(4)$ Å^3, $T = 200(2)$ K, space group $P\bar{1}$, $Z = 2$, μ(MoKα) = 2.651 mm^{-1}, 13712 reflections measured, 5577 independent reflections (R_{int} = 0.0495). The final R_1 values were 0.0307 ($I > 2\sigma(I)$). The final $wR(F^2)$ values were 0.0770 (all data). The goodness of fit on F^2 was 1.038.

Crystal data for **2**: $(C_{15}H_{16}N_7O_{10}Eu)_2 \cdot (C_4H_8O)_2 \cdot CH_2Cl_2$, $M = 1441.73$, triclinic, $a = 7.8867(16)$ Å, $b = 9.5923(19)$ Å, $c = 17.018(3)$ Å, $\alpha = 80.96(3)°$, $\beta = 87.80(3)°$, $\gamma = 81.94(3)°$, $V = 1258.7(4)$ Å^3, $T = 200(2)$ K, space group $P\bar{1}$, $Z = 1$, μ(MoKα) = 2.671 mm^{-1}, 9187 reflections measured, 5125 independent reflections (R_{int} = 0.0821). The final R_1 values were 0.0599 ($I > 2\sigma(I)$). The final $wR(F^2)$ values were 0.1579 (all data). The goodness of fit on F^2 was 1.060.

Positional parameters, hydrogen atom parameters, thermal parameters, bond distances and angles have been deposited as Supporting Information. Crystallographic data (excluding structure factors) for the structures reported in this paper have been deposited with the Cambridge Crystallographic Data Centre as a supplementary publication no. CCDC-776530 (**1**) and 776531 (**2**). Copies of the data can be obtained free of charge on application to CCDC, 12 Union Road, Cambridge CB21EZ, U.K. (fax: (+(44)1223−336−033; email: deposit@ccdc.cam.ac.uk).

(17) Sheldrick, G. M. *Acta Crystallogr., Sect. A* **2008**, *64*, 112–122.

TRLFS. The TRLFS titration experiments were performed using a stock solution of 7.30×10^{-6} mol/L Cm(III) (90.0% ^{248}Cm, 0.1% ^{247}Cm, 9.4% ^{246}Cm, 0.1% ^{245}Cm, 0.3% ^{244}Cm, and 0.4% ^{243}Cm) in 0.01 mol/L HClO$_4$. 27.4 μL of the Cm stock solution were evaporated to dryness and dissolved in 1000 μL of *n*-octan-1-ol. The initial Cm(III) concentration was 2.0×10^{-7} mol/L. Aliquots of a 1.00×10^{-2} mol/L 6-(3,5-dimethyl-1*H*-pyrazol-1-yl)-2,2′-bipyridine (dmpbipy) solution in *n*-octan-1-ol were added in portions of 10.0 and 30.0 μL, and spectra recorded after each addition. The dmpbipy concentration ranged from $0−2.75 \times 10^{-3}$ mol/L. For determination of the thermodynamic constants, TRLFS spectra were measured in the temperature range from 25 to 75 °C using a sample solution with [Cm] = 1.8×10^{-7} mol/L and [dmpbipy] = 1.3×10^{-3} mol/L. All TRLFS experiments were performed at low nitric acid concentrations ($< 10^{-3}$ M) to prevent protonation of the ligand.

Liquid−Liquid Extraction. dmpbipy's performance as an extracting agent was determined by measuring the distribution of ^{241}Am(III) and ^{152}Eu(III) between an organic phase containing dmpbipy and an aqueous phase containing nitric acid. ^{241}Am and ^{152}Eu are radionuclides with distinctive gamma lines which are easily detected by gamma counting. No sample preparation is required.

Organic phases were either solutions of the following:
(a)   0.05 mol/L dmpbipy in 1-octanol or
(b)   0.15 mol/L dmpbipy +0.5 mol/L 2-bromodecanoic acid in kerosene.

These were prepared by dissolving weighed amounts of dmpbipy and 2-bromodecanoic acid in the diluent (1-octanol or kerosene).

Aqueous phases were the following:
(a) ^{241}Am(III) + ^{152}Eu(III) in 0.01/0.1/1.0 mol/L HNO$_3$ + 1.0/1.9/0 mol/L NH$_4$NO$_3$ or
(b) ^{241}Am(III) + ^{152}Eu(III) in 0.01/0.02/0.05/0.1 mol/L HNO$_3$.

These were prepared by adding 10 μL of a stock solution of (60 kBq/mL ^{241}Am(III) + 100 kBq/mL ^{152}Eu(III) in 0.1 mo/L HNO$_3$) to 490 μL of HNO$_3$ or (HNO$_3$ + NH$_4$NO$_3$) with concentrations given above.

Equal volumes (0.5 mL each) of organic and aqueous phases (a) or (b) were contacted 30 min at 20 °C using an orbital shaker (2500/min). Samples were centrifuged to separate phases. ^{241}Am and ^{152}Eu activities were determined in 0.4 mL aliquots of each phase by gamma counting (Packard Cobra Auto Gamma 5003).

Am(III) and Eu(III) distribution ratios $D_{Am(III)}$ and $D_{Eu(III)}$ are $D_{M(III)}$ = [M(III)$_{org}$]/[M(III)$_{aq}$]. They are simply calculated from the organic phase and aqueous phase count rates or the respective radionuclide. The separation factor is $SF_{Am(III)/Eu(III)}$ = $D_{Am(III)}/D_{Eu(III)}$.

Distribution ratios usually are reproducible within ±20%.[18] Distribution ratios outside the range of $10^{-3} < D < 10^3$ may bear significantly larger errors and should be regarded with caution.

EXAFS Studies. For EXAFS measurement, a few mg of powdered compound **1** was mounted between self-adhesive Kapton film. The Am-dmpbipy complex was measured in solution. Thirty-five microliters of an Am stock solution (aqueous 0.5 M HNO$_3$ solution containing ^{243}Am 30MBq/mL and ^{241}Am 17MBq/mL, corresponding to 17 mmol/L Am) were gently heated in a glass vial to near dryness, without evolution of NO$_x$ gas, and then 300 μL 10 mmol/L dmpbipy in acetonitrile added; 250 μL of the resulting light pink colored solution were transferred to a 5 mm diameter polypropylene capped vial, the

(18) Hill, C.; Desreux, J. F.; Ekberg, C.; Espartero, A. G.; Galetta, M.; Modolo, G.; Geist, A.; Selucky, P.; Narbutt, J.; Madic, C. *Radiochim. Acta* **2008**, *96*, 259–264.

cap sealed shut with epoxy glue, and the sealed vial placed in the INE-Beamline standard sample containment chamber for measurement.

The EXAFS measurements were performed at the INE-Beamline for actinide research[19] at the Ångströmquelle Karlsruhe (ANKA), Karlsruhe Institute of Technology, Germany. The ANKA storage ring was operating at 2.5 GeV electron energy with a mean electron current of 120 mA. A pair of Ge(422) crystals (2d = 2.310 Å) for Am L3 studies and a Si(111) pair for the Eu L3 measurements were used in the double crystal monochromator (DCM). Higher harmonic radiation in the incident beam is suppressed by the two mirrors in the optics of the INE-Beamline and by detuning the parallel alignment of the DCM crystals to 70% of maximum photon flux peak intensity at the beginning of each scan. The incident intensity is measured by an Ar-filled or N_2-filled ionization chamber at ambient pressure for the Am and Eu experiments, respectively, and held constant by a digital MOSTAB feedback unit.

The Am L3 scans were calibrated against the first inflection point in the X-ray absorption near edge structure (XANES) spectrum of a Nb foil, defined as 18986 eV. The Eu L3 scans were calibrated in an analogous manner using a Fe foil (7112 eV). All scans were measured in standard fluorescence yield detection mode using a 5-pixel energy dispersive solid state Ge detector (Canberra LEGe). Four scans are collected and averaged for each sample.

Standard data reduction and least-squares fit techniques[20] using the ATHENA[21] and the UWXAFS[22] program packages were applied for EXAFS ($\chi(k)$) data analysis. The k^2-weighted $\chi(k)$ were obtained following pre-edge background subtraction, and normalization, μ_0 spline function fitting and subtraction, and conversion of energy to k using the energy of the white line intensity maximum to define the ionization energy (E_0). Hanning windows and k^2-weighting were used in the FT from k to R-space (Am k-range: 1.4 and 11 Å^{-1}; Eu k-range: 1.15 and 11 Å^{-1}). Least square fits of the EXAFS were performed in R-space (Am R-range: 1.3 and 2.6 Å; Eu R-range: 1.25 and 2.5 Å). Metric parameters describing the first coordination shell surrounding the central trivalent cations were obtained: coordination numbers (N), interatomic distances (R), mean square radial displacements or EXAFS Debye–Waller factors (σ^2), and relative shifts in ionization potential (ΔE_0). A third cumulant (σ^2) was added to the Am EXAFS fit model to better match oscillations at higher k-value. The amplitude reduction factor S_0^2 is held constant at 0.9. Theoretical scattering phase shift and backscattering amplitude functions used in the fits were obtained with the ab initio multiple-scattering code feff8.2[23] for the N1 atom coordinating Eu(III) calculated using the molecular arrangement shown in Figure 3. For Am, the central atom was simply switched from $Z = 63$ to $Z = 95$ for the calculation.

Results and Discussion

Metal Complex Synthesis. Dmpbipy was synthesized by a modified literature procedure[15] by treating 6-bromo-2,2′-bipyridine with potassium 3,5-dimethylpyrazolyl (K{(3,5-Me$_2$pz)(THF)}). After refluxing the reaction mixture for 5 days in diglyme, dmpbipy could be obtained in 81% yield after recrystallization from *n*-pentane (Scheme 2). The solid state structure of dmpbipy, which was established

(19) Denecke, M. A.; Rothe, J.; Dardenne, K.; Blank, H.; Hormes, J. *Phys. Scr.* **2005**, *T115*, 1001–1003.

(20) Rehr, J. J.; Albers, R. C.; Zabinsky, S. I. *Phys. Rev. Lett.* **1992**, *69*, 3397–3400.

(21) Ravel, B.; Newville, M. *J. Synchrotron Radiat.* **2005**, *12*, 537–541.

(22) Stern, E. A.; Newville, M.; Ravel, B.; Yacoby, Y.; Haskel, D. *Phys. B*. **1995**, *208&209*, 117–120.

(23) Ankudinov, A. L.; Ravel, B.; Rehr, J. J.; Conradson, S. D. *Phys. Rev. B* **1998**, *58*, 7565–7576.

Scheme 2
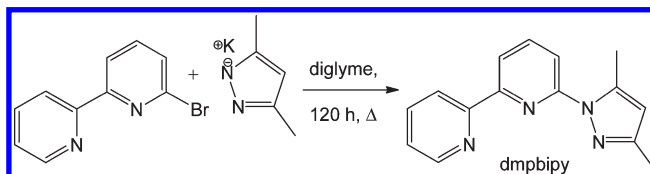
by single crystal X-ray diffraction (XRD, Figure 1), is in agreement with the obtained NMR data in solution. Some transition metal complexes of dmpbipy such [PtI(Me)$_3$-(dmpbipy)][24] and [ReBr(CO)$_3$(dmpbipy)][25] are known. In these compounds dmpbipy acts just as a bidentate ligand. To the best of our knowledge no f-metal compounds of dmpbipy were reported.
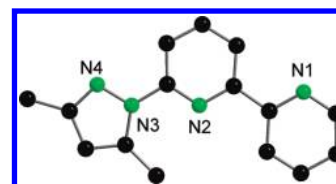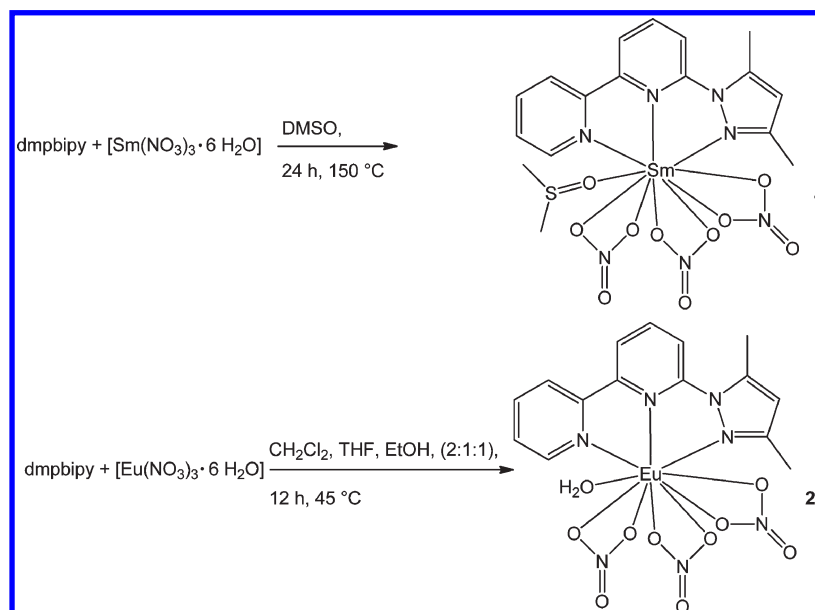

Figure 1. Solid-state structure of dmpbipy showing the atom labeling scheme, omitting hydrogen atoms.

Refluxing a 3:1 mixture of dmpbipy with [Sm(NO$_3$)$_3$·6H$_2$O] in DMSO for 1 day did not result in a complex with three ligands as it was previously observed with BTP. Instead the mono ligated compound [Sm(dmpbipy)-(NO$_3$)$_3$(DMSO)] (**1**) was obtained as yellow crystalline material after recrystallization from ethanol (Scheme 3). In contrast, BTP reacts with [Sm(NO$_3$)$_3$·6H$_2$O] to give the ionic complex of composition [Sm(BTP)$_3$] 1.5[Sm(NO$_3$)$_5$],[26] in which three BTP ligands are coordinated to the samarium atom. Obviously, the dmpbipy ligand does substitute the water molecules of the samarium atom but not the NO$_3^-$ anions. The new complex **1** has been characterized by standard analytical/spectroscopic techniques, and the solid state structure was established by single crystal XRD. The NMR data of complex **1** show one set of signals in solution. Although samarium(III) is paramagnetic, the signals are well resolved. Most characteristic are the signals of the methyl groups of the pyrazolyl ring, which are observed at δ (^{1}H) 2.20 ppm and 2.73 ppm; δ (^{13}C{^{1}H}) 13.6 ppm and 15.1 ppm. The aromatic region is less characteristic in the ^{1}H NMR spectrum. In comparison to non-coordinated dmpbipy, the signals are shifted slightly. In general, a slight downfield shift of the signals of the aromatic region is observed.

Compound **1** crystallizes in the triclinic space group $P\overline{1}$ having two molecules of **1** in the unit cell (Figure 2). The coordination polyhedron of complex **1** is formed by the tridentate dmpbipy ligand, three NO$_3^-$ anions, and one DMSO molecule resulting in a 10-fold coordinated Sm atom. The Sm–O bond distances of the nitro groups range within the expected area of 2.509(3) Å to 2.569(3) Å. The dmpbipy ligand is slightly twisted resulting in a torsion angle of N1–N2–N3–N4 of 20.84(4)°. The bite angles of

(24) Gelling, A.; Orrell, K. G.; Osborne, A. G.; Šik, V. *Polyhedron* **1996**, *15*, 3203–3210.

(25) Gelling, A.; Orrell, K. G.; Osborne, A. G.; Šik, V.; Hursthouse, M. B.; Coles, S. J. *J. Chem. Soc., Dalton Trans.* **1996**, 203–209.

(26) Drew, M. G. B.; Guilaneux, D.; Hudson, M. J.; Iveson, P. B.; Russell, M. L.; Madic, C. *Inorg. Chem. Commun.* **2001**, *4*, 12–15.

Scheme 3

the dmpbipy ligand are N1−Sm−N2 62.92(9)°, N1−Sm−N4 124.41(9)°, and N2−Sm−N4 61.66(9)°. Interestingly, there is no significant difference in the Sm−N bond length of the outer six membered pyridine ring (Sm−N1 2.587(3) Å) and the five membered pyrazolyl ring (Sm−N4 2.589(3) Å). A comparison of compound **1** with the cation of [Sm(BTP)$_3$]·1.5[Sm(NO$_3$)$_5$] does not show any significant difference in the Sm−N bond distances, for example, the average Sm−N bond length of the pyridine ring in [Sm(BTP)$_3$]$^{3+}$ is 2.574 Å.[26]

To access an europium dmpbipy complex, different reaction conditions compared to the synthesis of **1** were necessary. Reaction of dmpbipy with Eu(NO$_3$)$_3$·6H$_2$O in a 3:1 molar ratio again resulted in a mono ligated complex of composition [Eu(dmpbipy)(NO$_3$)$_3$(H$_2$O)] (**2**) (Scheme 3). As observed for compound **1** the NO$_3^-$ anions are not substituted by the dmpbipy ligand resulting in a neutral species. Since compound **2** could be synthesized and crystallized

in the absence of strong Lewis-base, one of the water molecules remained on the center atom. Complex **2** has been characterized by standard analytical/spectroscopic techniques, and the solid-state structure was established by single crystal XRD. As result of the paramagnetic metal center only broad signals are observed in the ^{1}H NMR spectrum of compound **2**.

Compound **2** crystallizes in the triclinic space group $P\bar{1}$ having two molecules of **2**, two molecules of THF, and one molecule of CH$_2$Cl$_2$ in the unit cell. There is to the best of our knowledge no solid state structure of a BTP europium complex known. The coordination structure of europium in compound **2** is shown in Figure 3. As in compound **1**, only one equivalent of dmpbipy is attached to the metal center. The coordination polyhedron of complex **2** is thus formed by the tridendate dmpbipy ligand, three NO$_3^-$ anions, and one molecule of water. As observed for compound **1** a 10-fold coordinated metal atom is obtained. The Eu−N bond
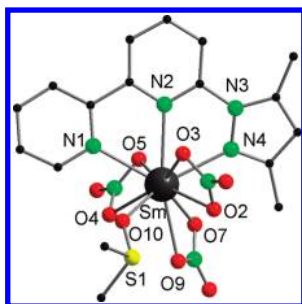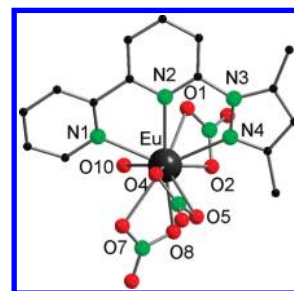

Figure 2. Solid-state structure of **1** showing the atom labeling scheme, omitting hydrogen atoms. Selected bond lengths [Å] or angles [deg]: Sm−O2 2.534(3), Sm−O3 2.554(3), Sm−O4 2.549(3), Sm−O5 2.509(3), Sm−O7 2.553(3), Sm−O9 2.569(3), Sm−O10 2.372(3), Sm−N1 2.587(3), Sm−N2 2.613(3), Sm−N4 2.589(3); O2−Sm−N1 131.94(10), O3−Sm−N1 87.17(10), O4−Sm−N1 71.00(9), O5−Sm−N1 71.18(9), O7−Sm−N1 134.16(10), O9−Sm−N1 131.51(10), O10−Sm−N1 72.73(9), O2−Sm−N4 71.19(10), O3−Sm−N4 75.75(11), O4−Sm−N4 129.69(10), O5−Sm−N4 86.90(10), O7−Sm−N4 73.35(10), O9−Sm−N4 103.52(10), O10−Sm−N4 145.58(10), O2−Sm−N2 108.01(9), O3−Sm−N2 67.25(9), O4−Sm−N2 113.41(9), O5−Sm−N2 70.45(9), O7−Sm−N2 118.97(9), O9−Sm−N2 164.94(10), O10−Sm−N2 122.19(10), N1−Sm−N2 62.92(9), N1−Sm−N4 124.41(9), N2−Sm−N4 61.66(9).

Figure 3. Solid-state structure of **2** showing the atom labeling scheme, omitting hydrogen atoms. Selected bond lengths [Å] or angles: Eu−N1 2.495(6), Eu−N2 2.575(6), Eu−N4 2.494(6), Eu−O1 2.521(5), Eu−O2 2.464(5), Eu−O4 2.468(5), Eu−O5 2.559(5), Eu−O7 2.468(5), Eu−O8 2.459(5), Eu−O10 2.409(6); O1−Eu−N1 96.3(2), O2−Eu−N1 138.1(2), O4−Eu−N1 73.5(2), O5−Eu−N1 119.0(2), O7−Eu−N1 77.2(2), O8−Eu−N1 122.9(2), O10−Eu−N1 71.0(2), O1−Eu−N4 69.68(2), O2−Eu−N4 72.8(2), O4−Eu−N4 80.7(2), O5−Eu−N4 72.2(2), O7−Eu−N4 141.1(2), O8−Eu−N4 111.8(2), O10−Eu−N4 139.2(2), O1−Eu−N2 67.9(2), O2−Eu−N2 112.5(2), O4−Eu−N2 68.8(2), O5−Eu−N2 106.9(2), O7−Eu−N2 132.6(2), O8−Eu−N2 172.9(2), O10−Eu−N2 1123.0(2), N1−Eu−N2 63.7(2), N1−Eu−N4 124.8(2), N2−Eu−N4 61.3(2).

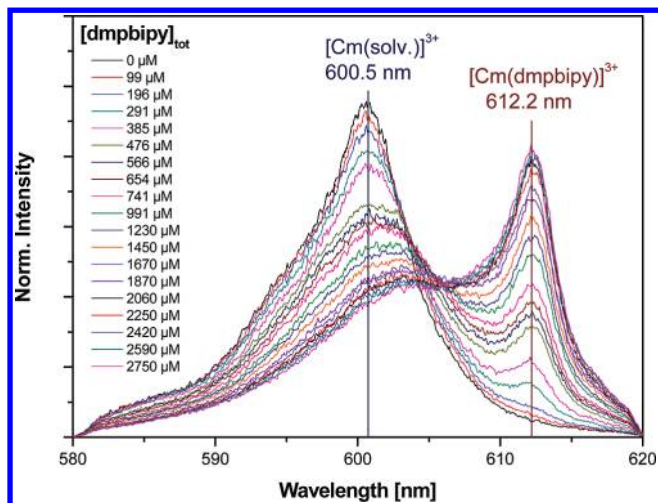**Figure 4.** Normalized fluorescence spectra of Cm(III) in *n*-octan-1-ol with increasing dmpbipy concentration. [Cm(III)] = 2×10^{-7} mol/L; [dmpbipy] = $0-2.75 \times 10^{-3}$ mol/L.

lengths of the outer rings of the dmpbipy are within a similar range (Eu−N1 2.495(6) Å and Eu−N4 2.494(6) Å), whereas the distance to the central ring is as result of sterical reasons about 0.08 Å longer (Eu−N2 2.575(6) Å). The bite angles of the dmpbipy ligand are N1−Eu−N2 63.7(2)°, N1−Eu−N4 124.8(2)°, and N2−Eu−N4 61.3(2)°. As a result of the smaller ion radius of Eu(III) compared to Sm(III) the N1−N2−N3−N4 torsion angle of 6.49(5)° of the dmpbipy ligand is smaller than in compound **1**.

TRLFS. Figure 4 depicts fluorescence spectra of Cm(III) resulting from the $^6D'_{7/2} \rightarrow {}^8S'_{7/2}$ transition in the presence of increasing amounts of dmpbipy in *n*-octan-1-ol. The spectra are normalized to the same peak area for better comparison. The spectrum of Cm in *n*-octan-1-ol is measured as a reference and displays an emission band at 600.5 nm. In the presence of increasing dmpbipy concentration, a Cm-dmpbipy complex is formed with an emission maximum at 612.2 nm; the emission band of the solvated Cm complex ([Cm(solv.)]$^{3+}$) decreases simultaneously. The fluorescence spectrum of the Cm-dmpbipy complex shows a strong bathochrome shift of the emission band compared to the solvated Cm(III) and a distinct shoulder at the blue flank resulting from a strong ligand field splitting of the first excited state caused by strong complexing ligands. Upon further addition of ligand the fraction of Cm-dmpbipy increases but no other species is observed. These results show that exclusively one Cm-dmpbipy species is formed at [ligand]/ [metal ion] ratios up to 13750 ([L]= 2.75×10^{-3}).

Each spectrum was analyzed by peak deconvolution using the fluorescence spectra of the two single components ([Cm-(solv.)]$^{3+}$ and Cm-dmpbipy). The resulting speciation diagram is shown in Figure 5. At low dmpbipy concentration, the [Cm(solv.)]$^{3+}$ complex is the dominant species. With increasing ligand concentration the fraction of the solvated species decreases, whereas the Cm-dmpbipy complex is formed. As shown in Figure 5 Cm-dmpbipy becomes the dominating species at ligand concentrations > 1.7×10^{-3} mol/L.

To ascertain the stoichiometry of the formed Cm-dmpbipy complex, slope analysis of the titration results was performed using the following reaction:
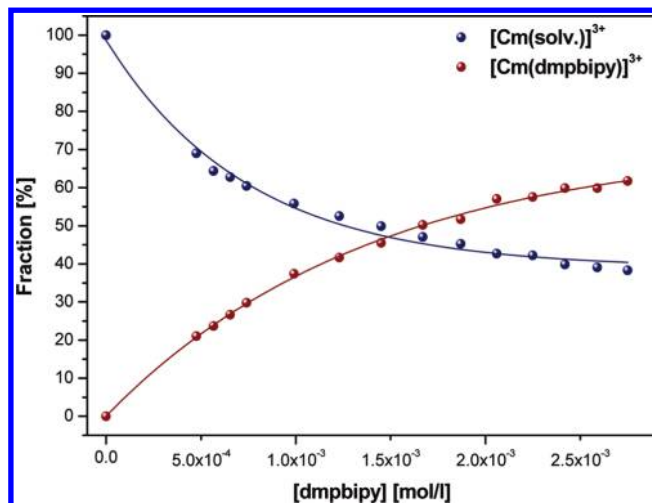
$$Cm^{3+} + n \text{ dmpbipy} \rightleftharpoons [Cm(\text{dmpbipy})_n]^{3+} \quad (1)$$

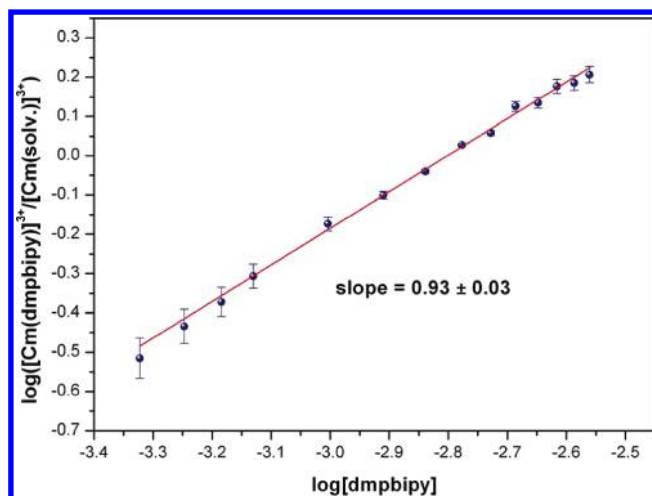**Figure 5.** Distribution of Cm(III) species in *n*-octan-1-ol as a function of the dmpbipy concentration.

Figure 6. Double logarithmic plot of [Cm(dmpbipy)$_n$]$^{3+}$/[Cm(solv.)]$^{3+}$ concentration ratio versus free dmpbipy concentration.

It follows that

$$\log\left(\frac{[Cm(dmpbipy)_n]^{3+}}{[Cm(solv.)]^{3+}}\right) = \log K + n \log[dmpbipy]$$

(2)

According to eq 2, there is a linear correlation between the logarithm of the concentration ratio [Cm-(dmpbipy)$_n$]$^{3+}$/[Cm(solv.)]$^{3+}$ and the logarithm of the free dmpbipy concentration with a slope of *n*. The double logarithmic plot of the spectroscopically determined concentration ratios of the different species in solution at various ligand concentrations is shown in Figure 6. A slope of 0.93 ± 0.03 was obtained by linear regression, which confirms the formation of a 1:1 Cm-dmpbipy complex. Coordination of the trivalent cation by a single tridentate dmpbipy ligand observed in X-ray crystallographic results of the lanthanide complexes is retained in solution; higher complexed species, such as 1:2 and/ or 1:3 complexes known for BTPs,[9,10] were not observed even at very high ligand concentration (up to 2.75×10^{-3} mol/L).
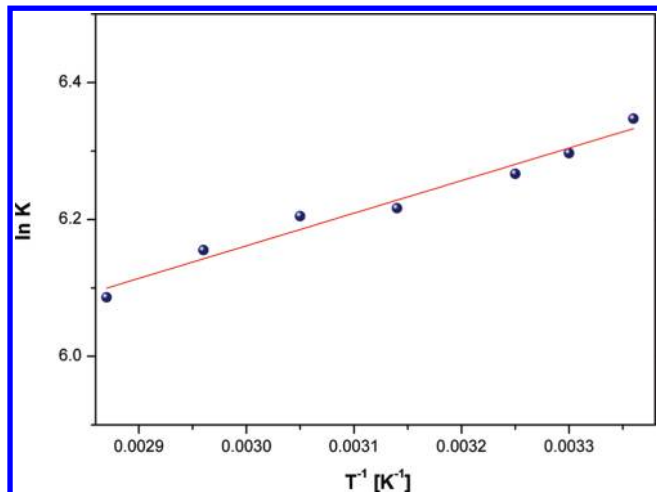
Figure 7. Temperature dependency of the stability constants for the 1:1 Cm-dpmpbipy complex in *n*-octan-1-ol in the temperature range from 25−75 °C ([Cm(III)] = 1.8×10^{-7} mol/L; [dmpbipy] = 1.3×10^{-3} mol/L).

Table 1. Thermodynamic Data of the Formation of 1:1 Cm-dmpbipy in *n*-octan-1-ol

	ΔH [kJ/mol]	ΔS [J/mol·K]	ΔG (20 °C) [kJ/mol]
1:1 Cm-dmpbipy	-4.0 ± 0.3	39.3 ± 0.9	-15.5 ± 1.1

The conditional stability constant log K of the 1:1 Cm-dmpbipy complex in *n*-octan-1-ol (25 °C) was calculated from the species distribution obtained spectroscopically according to eq 3:

$$K = \frac{[Cm(dmpbipy)]^{3+}}{[Cm(solv.)]^{3+} \cdot [dmpbipy]} \quad (3)$$

An average value log K = 2.80 ± 0.02 was obtained, which is fairly low.

To determine the Gibbs free energy, enthalpy, and entropy of reaction for the complex formation in *n*-octan-1-ol, temperature dependent stability constants were determined in the temperature range from 25 to 75 °C. The stability constants of the 1:1 Cm-dmpbipy complex as a function of the reciprocal temperature are shown in Figure 7. The thermodynamic data were determined by least-squares linear fits of the temperature dependent stability constants to the van't Hoff equation. The results are summarized in Table 1.

These results show that the formation of 1:1 Cm-dmpbipy is driven by enthalpy and entropy, although the absolute values of ΔH and ΔS are low.

Liquid−Liquid Extraction. The performance of dmpbipy as a selective An(III) extracting agent was tested with liquid−liquid distribution measurements. Extraction efficiency was characterized by Am(III) and Eu(III) distribution ratios, $D_{Am(III)}$ and $D_{Eu(III)}$, with $D_{M(III)}$ = [M(III)$_{org}$]/[M(III)$_{aq}$], and the separation factor, $SF_{Am(III)/Eu(III)}$ = $D_{Am(III)}/D_{Eu(III)}$. A component's extraction ($D > 1$) and back extraction ($D < 1$) should be tunable simply by changing an aqueous phase concentration (e.g., acidity, ionic strength). Furthermore, good selectivity (high SF) is desirable.

Dmpbipy has a solubility of approximately 0.05 mol/L in 1-octanol and does not extract Am(III) or Eu(III) from
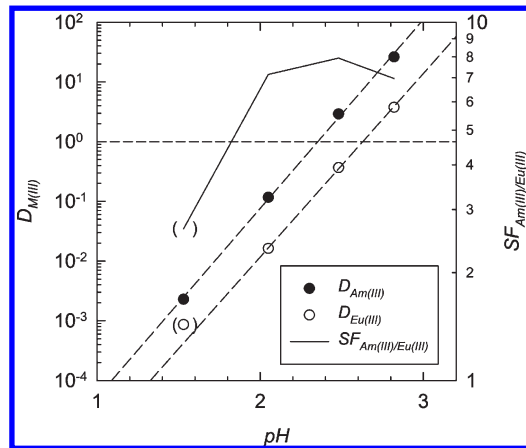

Figure 8. Extraction of Am(III) and Eu(III) from HNO$_3$ into 0.15 mol/L dmpbipy +0.5 mol/L 2-bromohexanoic acid in kerosene, T = 20 °C. Am(III) and Eu(III) distribution ratios (left axis) and separation factors (right axis) as a function of aqueous equilibrium pH.

HNO$_3$ or acidic NH$_4$NO$_3$ solutions by solvation according to eq 4.

$$M^{3+}_{aq} + 3NO_3^-{}_{aq} + nL_{org} = M(NO_3)_3 \cdot nL_{org} \quad (4)$$

In this case, Am(III) and Eu(III) distribution ratios are $< 10^{-3}$.

This ligand was found to extract trivalent cations as bromodecanoates; a solution of 0.15 mol/L dmpbipy +0.5 mol/L 2-bromohexanoic acid in kerosene extracts Am(III) from solutions of pH > 2.4 with limited selectivity over Eu(III); $SF_{Am(III)/Eu(III)} \approx 8$ (Figure 8), according to eq 5.

$$M^{3+}_{aq} + 3HA_{org} + nL_{org} = MA_3 \cdot nL_{org} + 3H^+_{aq} \quad (5)$$
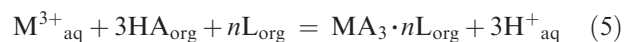
Extraction occurs at higher pH; lower pH shifts the equilibrium to the left. Slopes of 3.2 and 3.1, which are close to the expected value of 3, were observed for log D *versus* pH for Am(III) and Eu(III), respectively (disregarding the value at pH = 1.5 for Eu(III)). That the measured equilibrium pH values were higher than expected from the initial HNO$_3$ concentrations used (e.g., pH = 2.48 was measured for 0.02 mol/L HNO$_3$, which would correspond to pH = 1.7), indicates dmpbipy was partly protonated under these conditions. For this reason, the number of dmpbipy molecules present in the extracted complex (n in eq 5) could not be determined by slope analysis. We assume from the XRD, TRLFS, and EXAFS (cf. below) results that $n = 1$.

EXAFS Analysis. The Eu and Am L3 edge k^2-weighted EXAFS and corresponding Fourier transformed (FT) spectra are shown in Figure 9 and 10, respectively. The results from fits of the data to the EXAFS equation are listed in Table 2, and the fit curves are also depicted in Figure 9 and 10.

The FT spectrum for compound **1** shows little intensity above the first coordination shell with its maximum located at 1.96 Å (uncorrected for phase shift). The fit results for the first coordination shell are in accordance with the structure analysis results for compound **1** reported above. Both the bond distance and the coordination number from the EXAFS analysis are the same as the

Table 2. Metric Parameters Obtained from Fits of R-Space Data Shown in Figures 9 and 10[a]

sample	shell	R [Å]	N	σ^2 [Å^2]	σ^3 [Å^3]	ΔE [eV]	r-factor
1	Eu−N/O	2.50(1)	10(1)	0.006(2)		9.8(8)	0.01
Am- dmpbipy	Am−N/O	2.48(3)	10(1)	0.006(2)	−0.0015(6)	3(2)	0.003

[a] Values in parentheses give the statistical error for that parameter's fit result last significant digit.
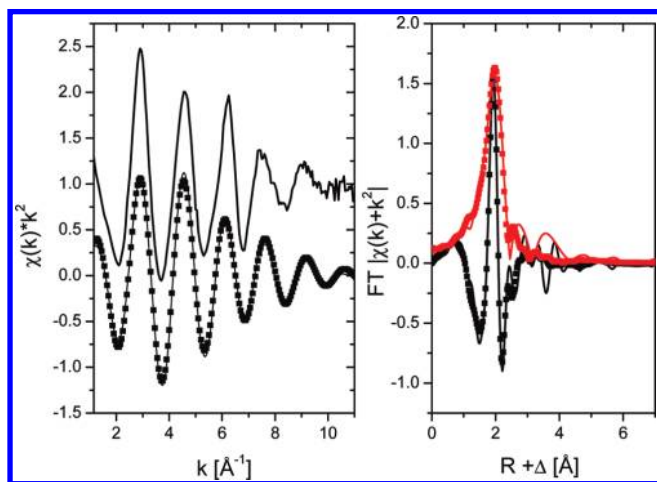

Figure 9. Left: k^2-weighted Eu L3 EXAFS (experimental, filtered, and fitted data). Right: corresponding Fourier transform (FT, magnitude and imaginary part shown) for compound **1**. The experimental EXAFS is shifted along the y-axis for clarity. Experimental and filtered data are shown as lines, and fit curves as symbols.
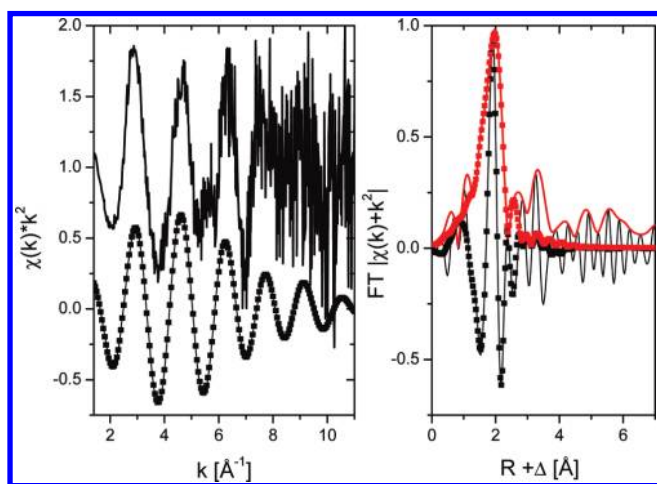

Figure 10. Left: k^2-weighted Am L3 EXAFS (experimental, filtered, and fitted data). Right: corresponding Fourier transform (FT, magnitude and imaginary part shown) for Am-dmpbipy in solution (see text for details). Experimental EXAFS is shifted along the y-axis for clarity. Experimental and filtered data are shown as lines and fit curves as symbols.

average distance for the 10 O/N atoms determined from XRD (2.492 Å) to within experimental error. FT intensity for the second shell composed of the N3 atom, C atoms adjacent to the ligating N atoms of dmpbipy, and N atoms of the coordinating nitrate groups is essentially non-existent. Analysis of scattering pathways from the Feff calculations reveal that a number of scattering paths associated with this shell interfere destructively. The atoms belonging this shell are at different distances; those atoms of the ligand and those belonging to the nitrate molecules have approximately a 0.5 Å difference in their

Eu−N/C distances. The interatomic Eu−N distances for the nitrate molecules range over nearly 0.5 Å. In addition there are numerous 3-legged multiple scattering paths with similar effective distances (between 3.31 and 3.38 Å). These numerous oscillations lead to destructive interference of their associated EXAFS amplitude. The other feature seen in the FT near 4 Å is likely from the distal O atoms of the nitrate groups, enhanced in intensity through the lensing effect of its collinear N atom.[27]

The quality of the data for the Am-dmpbipy solution sample is much poorer. However, it has the same general features in the FT spectrum, including the peak near 4 Å indicating coordinating nitrate ions. The fit result to the first shell is nearly identical to that for the solid Eu-dmpbipy compound. The EXAFS data is consistent with a similar coordination geometry of the trivalent cation in solution. We assume that there is not more than one dmpbipy molecule bound to the Am(III) cation. If additional dmpbipy ligands were bound, observation of significant intensity of N/C atoms from the second shell would be expected, as the ratio of ligand to nitrate ions would in this case change drastically, and the destructive interference of the signal from the second shell would be not complete.

Note that the static disorder associated with the Am-dmpbipy coordination is apparently higher than that in the Eu-dmpbipy compound **1**. We had to include a higher order of the EXAFS Debye−Waller factor or third cumulant[28] to successfully model the first shell frequency at higher k values, which accounts for asymmetry in the near-neighbor distribution around the Am cation, i.e., for a non-Gaussian radial pair distribution function.

Conclusion

In this study a N donor complexing ligand was synthesized, which had a defined variation from the partitioning ligand BTP structure: replacing a 1,2,4-triazine ring with a pyridine and the other triazine with a smaller five membered pyrazole. The extraction performance and selectivity of this dmpbipy ligand for trivalent actinide cations over lanthanides was found to be poor, especially at low pH values. We suggest that the ligand is protonated and thus coordination of the ligand to the metal center is hampered. The equilibrium constant for curium complex formation with dmpbipy was determined to be several orders of magnitude smaller than that of BTP[29−31] and similar to that for nitrate. Although this ligand is therefore not a suitable ligand for a partitioning process, where separations must be performed in nitric acid solution, we have gained some deeper insight into the

(27) Denecke, M. A. *Coord. Chem. Rev.* **2006**, *250*, 730–754.

(28) Traquada, J. M.; Ingalls, R. *Phys. Rev. B* **1983**, *28*, 3520.

(29) Trumm, S.; Panak, P. J.; Geist, A.; Fanghänel, T. *Eur. J. Inorg. Chem.* **2010**, 3022–3028.

(30) Colette, S.; Amekraz, B.; Madic, C.; Berthon, L.; Cote, G.; Moulin, C. *Inorg. Chem.* **2002**, *41*, 7031–7041.

(31) Hubscher-Bruder, V.; Haddaoui, J.; Bouhroum, S.; Arnaud-Neu, F. *Inorg. Chem.* **2010**, *49*, 1363–1371.

coordination behavior of modified BTP ligands. The present investigations have shown that TRLFS is a very sensitive speciation method that can yield valuable information concerning the thermodynamic parameters of complex formation including complex strength. This can be used as a versatile tool in ligand design and development by providing direct feedback to the question if it is worthwhile to alter/ optimize a selected ligand for partitioning applications. For example, if the formation constant is found to be favorable but the solubility is poor, activity should then be improved by synthesizing a more lipophilic ligand. This can potentially save valuable time in the laboratory.

Future efforts will concentrate on designing and synthesizing ligands with less dramatic, but systematic, variation from the BTP structure and applying this sort of spectroscopic screening to judge the promise of the ligand extraction performance. Furthermore, N 1s near-edge X-ray fine structure, high resolution X-ray emission, and resonant inelastic X-ray scattering spectroscopic tools will be applied to evaluate the electronic structure of the An(III) complexes versus their Ln(III) homologues, to understand differences in their bonding properties. Such information may help "fine tune" the ligand design or process parameters such as solvent dielectric strength.

Supporting Information Available: X-ray crystallographic files in CIF format for the structure determinations of dmpbipy, **1**, and **2**. This material is available free of charge via the Internet at http://pubs.acs.org.